# Energetics and Structure of Nicotinic Acid (Niacin)

**Elsa M. Gonçalves,[†] Carlos E. S. Bernardes,[†,‡] Hermínio P. Diogo,[‡] and Manuel E. Minas da Piedade*,[†]**

*Departamento de Química e Bioquímica, Faculdade de Ciências, Universidade de Lisboa, 1649-016 Lisboa, Portugal, and Centro de Química Estrutural, Complexo Interdisciplinar, Instituto Superior Técnico da Universidade Técnica de Lisboa, 1049-001 Lisboa, Portugal*

*Received: February 18, 2010; Revised Manuscript Received: March 18, 2010*

The standard molar enthalpies of formation and sublimation of crystalline (monoclinic, space group $P2_1/c$) nicotinic acid (NA), at 298.15 K, were determined as $\Delta_f H^\circ_m$(NA, cr) = −344.7 ± 1.2 kJ·mol$^{-1}$ and $\Delta_{sub} H^\circ_m$(NA) = 112.1 ± 0.5 kJ·mol$^{-1}$ by using combustion calorimetry, drop-sublimation Calvet microcalorimetry, and the Knudsen effusion method. The experimental determinations were all based on a sample of NIST Standard Reference Material 2151, which was characterized in terms of chemical purity, phase purity, and morphology. From the above results, $\Delta_f H^\circ_m$(NA, g) = −232.6 ± 1.3 kJ·mol$^{-1}$ could be derived. On the basis of this value and on published experimental data, the enthalpy of the isodesmic reaction nicotinic acid(g) + benzene(g) → benzoic acid(g) + pyridine(g) was calculated as −3.6 ± 2.7 kJ·mol$^{-1}$ and compared with the corresponding predictions by the B3LYP/cc-pVTZ (−3.6 kJ·mol$^{-1}$), B3LYP/aug-cc-pVTZ (−3.7 kJ·mol$^{-1}$), B3LYP/6-311++G(d,p) (−4.2 kJ·mol$^{-1}$), G3MP2 (−4.3 kJ·mol$^{-1}$), and CBS-QB3 (−4.0 kJ·mol$^{-1}$) quantum chemistry models. The excellent agreement between the experimental and theoretical results supports the reliability of the $\Delta_f H^\circ_m$(NA, cr), $\Delta_{sub} H^\circ_m$(NA), and $\Delta_f H^\circ_m$(NA, g) recommended in this work. These data can therefore be used as benchmarks for discussing the energetics of nicotinic acid in the gaseous and crystalline states and, in particular, to evaluate differences imparted to solid forms by the production and processing methods. Such differences are perhaps at the root of the significant inconsistencies found between the published enthalpies of sublimation of this important active pharmaceutical ingredient and thermochemical standard. The molecular packing in the crystalline phase studied in this work was also discussed and its influence on the molecular structure of nicotinic acid was analyzed by comparing bond distances and angles published for the solid state with those predicted by the B3LYP/cc-pVTZ method. No advantage in terms of accuracy of the structural predictions was found by the use of the larger aug-cc-pVTZ or 6-311++G(d,p) basis sets.

## Introduction

Nicotinic acid (NA, CAS number [59-67-6]), pyridine-3-carboxylic acid, also known as niacin or vitamin $B_3$, is a water-soluble vitamin, that is credited to have been synthesized for the first time by Huber, in 1867.[1] It is an indispensable nutrient for humans and animals, and has been widely used as an additive in food, forage, and cosmetics.[2,3] It has also found important pharmacological applications, particularly in the treatment of hypercholesterolemia and atherosclerosis.[4,5] The world demand for nicotinic acid and its derivatives has been steadily rising from 8500 t per year in the 1980s to 22000 t in the 1990s and, more recently, 35000−40000 t.[6−8]

Nicotinic acid is often employed as a solid, and it is well-known that the physical properties of organic molecular solids may be affected by the methods of production and processing, with a possible impact on the end-use applications. For example, the manufacturing of solid dosage forms normally involves the purification of the active pharmaceutical ingredient (API) by crystallization from solution, followed by grinding and compaction. Any of these processes can influence the crystallinity, size, morphology, and energetics (lattice and surface energies) of the API particles, and even the nature of the obtained phase if different polymorphs are possible. These aspects dictate, in turn, the dissolution rate of the drug, ultimately affecting its therapeutic window.[9−11]

We have long been interested in the study of the relationship between the structure and energetics of individual molecules,[12] and more recently on how intermolecular forces determine their packing in the solid state, the lattice energy of the crystals,[13−15] or the relative stability of different polymorphs that may coexist under the same temperature and pressure conditions.[16] The importance of NA

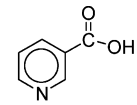


Nicotinic acid (NA)

both as an API and as a standard reference material for the measurement of enthalpies of combustion[17] makes it an attractive candidate for these types of studies, in particular, since it is not clear from the literature how strongly changes in crystallinity, morphology, particle size distribution, etc., associated with the methods of preparation and processing may influence the thermodynamic stability of a given sample. Thus, for example, while a preformulation study carried out by thermogravimetry showed no significant effect of compaction and grinding on the kinetics of nicotinic acid sublimation,[18] the values of the standard

* To whom correspondence should be addressed. E-mail: memp@fc.ul.pt.
† Universidade de Lisboa.
‡ Instituto Superior Técnico da Universidade Técnica de Lisboa.

10.1021/jp101490b 
Published on Web 04/08/2010

molar enthalpies of sublimation at 298.15 K, $\Delta_{sub}H^{\circ}_{m}$(NA), published over a period of 18 years span a range of ~20 kJ·mol$^{-1}$.[19−22] In contrast, the three independent determinations of the standard molar enthalpy of formation of crystalline nicotinic acid, $\Delta_{f}H^{\circ}_{m}$(NA, cr), reported over a period of 24 years diverge by no more than ±0.5 kJ·mol$^{-1}$.[21,23,24] It is worth mentioning that a fourth and recent measurement led to a $\Delta_{f}H^{\circ}_{m}$(NA, cr) value differing by 288 kJ·mol$^{-1}$ from the average of all the previous ones.[25] This must not be considered, however, because the discrepancy was later found by the authors to be due to problems with the calorimetric apparatus and the result was discarded.[26]

Inconsistencies in $\Delta_{f}H^{\circ}_{m}$(NA, cr) and $\Delta_{sub}H^{\circ}_{m}$(NA), arising from sample variability, necessarily affect $\Delta_{f}H^{\circ}_{m}$(NA, g), which is derived as a sum of the first two quantities. Analysis of the original literature revealed that only in one case[21] were both $\Delta_{f}H^{\circ}_{m}$(NA, cr) and $\Delta_{sub}H^{\circ}_{m}$(NA) measured in the same laboratory, and presumably with the same sample. We therefore felt that, before embarking on further studies of the relationship between the structure and energetics of nicotinic acid, the two basic thermodynamic properties $\Delta_{f}H^{\circ}_{m}$(NA, cr) and $\Delta_{sub}H^{\circ}_{m}$(NA), which reflect the lattice energy, should be obtained using a single and well-characterized sample and put on a firmer basis.

This work describes the redetermination of the standard molar enthalpies of formation and sublimation of nicotinic acid by using combustion calorimetry, drop-sublimation Calvet microcalorimetry, and the Knudsen effusion method. The experimental determinations were all based on a sample of NIST SRM 2151, which was characterized in terms of chemical purity, phase purity, and morphology. Density functional theory (DFT),[27] Gaussian-3 theory with second-order Møller−Plesset (G3MP2),[28] and complete basis set - quadratic Becke3 (CBS-QB3)[29,30] calculations were also applied to help in the assessment of the internal consistency of the obtained experimental results. Finally, the crystal packing of the nicotinic acid form studied in this work and its influence on the molecular structure were also analyzed using the predictions of the DFT models for an isolated molecule in the gas phase as a reference.

## Materials and Methods

**General.** Elemental analyses were carried out on a Fisons Instruments EA1108 apparatus. Diffuse reflectance infrared Fourier-transform (DRIFT) spectroscopy measurements were performed in the range 400−4000 cm$^{-1}$ using a Nicolet 6700 spectrometer. The resolution was 2 cm$^{-1}$, and the samples were ~5% (w/w) nicotinic acid in KBr. The $^{1}$H NMR and $^{13}$C NMR spectra were obtained in DMSO-$d_6$, (Aldrich 99.9% containing 0.03% v/v TMS) at ambient temperature, on a Bruker Ultrashield 400 MHz spectrometer. GC-MS experiments were performed on an Agilent 6890 gas chromatograph equipped with an Agilent 7683 automatic liquid sampler coupled to an Agilent 5973 N quadrupole mass selective detector. An HP-5 column (5% diphenyl/95% dimethylpolysiloxane; 28.7 m × 0.25 μm I.D., 250 μm film thickness) was used. The sample was dissolved in methanol (Fisher Scientific, HPLC grade, 99.99%), and the injection volume was 1 μL. The carrier gas was helium maintained at a constant pressure of 1.19 bar and with a flow rate of 1.3 mL·min$^{-1}$. A programmed temperature vaporization injector with a septumless sampling head having a baffled liner (Gerstel) operating in the splitless mode was employed. The inlet temperature was set to 523 K, and the oven temperature was programmed as follows: 353 K for 1 min, ramp at 5 K·min$^{-1}$ to 373 K, and finally ramp to 573 at 15 K·min$^{-1}$, for a total 18.33 min running time. The transfer line, ion source, and quadrupole analyzer were maintained at 553, 503, and 423 K, respectively. A solvent delay of 4 min was selected. Electron ionization mass spectra in the range 35−550 *m*/*z* were recorded in the full-scan mode, with 70 eV electron energy and an ionization current of 34.6 μA. Data recording and instrument control were performed by using the MSD ChemStation software from Agilent (G1701CA; version C.00.00). The identity of the analyzed compound was assigned by comparison of the mass-spectrometric results with the data in Wiley's reference spectral databank (G1035B, Rev D.02.00), and its purity was calculated from the normalized peak areas, without using correction factors to establish abundances. X-ray powder diffraction analyses were carried out on a Philips PW1730 diffractometer, with automatic data acquisition (APD Philips v.35B), operating in the $\theta-2\theta$ mode. The apparatus had a vertical goniometer (PW1820), a proportional xenon detector (PW1711), and a graphite monocromator (PW1752). A Cu Kα radiation source was used. The tube amperage was 30 mA and the tube voltage 40 kV. The diffractograms were recorded at ~293 K in the range $10° \le 2\theta \le 40°$. Data were collected in the continuous mode, with a step size of 0.015°($2\theta$) and an acquisition time of 1.5 s/step. The samples were mounted on an aluminum sample holder. The indexation of the powder patterns was performed using the program Checkcell.[31] Scanning electron microscopy (SEM) images of Au/Pd-sputtered samples were recorded in high vacuum, using a FEI ESEM Quanta 400 FEG apparatus, with a resolution of 2 nm. The electron beam voltage was set to 10 kV.

**Materials.** A nicotinic acid sample from NIST (standard reference material 2151),[32] without further purification, was used in all thermodynamic measurements. Elemental analysis for $C_6H_5O_2N$: expected C 58.54%, H 4.10%, N 11.38%; found C 58.26%, H 3.91%, N 11.15% (average of two determinations). DRIFT (KBr, main peaks): $\tilde{\nu}$/cm$^{-1}$ = 3085, 3072 ($\nu_{C-H}$); 2821, 2445, 1948 ($\nu_{N\cdots H\cdots O}$); 1709 ($\nu_{C=O}$, −COOH); 1596, 1583 ($\nu_{C=C}$, $\nu_{C=N}$, ring); 1495 ($\delta_{O-H\cdots N}$, in plane); 1418 ($\nu_{C=C}$, $\nu_{C=N}$, ring); 1324 ($\delta_{O-H}$, in plane); 1303 ($\nu_{C-O}$, −COOH); 1186, 1139, 1115 ($\beta_{C-H}$, in plane), 1089 ($\delta_{O-H\cdots N}$, out of plane); 1041, 1033 ($\nu$ ring breathing); 955 ($\delta_{C-H\cdots O}$, out of plane); 831; 811, 751, 695 ($\gamma_{C-H}$, out of plane); 682 ($\delta_{COO}$, −COOH); 642, 498 ($\delta_{ring}$, in plane deformation). The assignments were based on those given by Taylor,[33] Goher and Drátovský,[34] and Hudson et al.[35] $^{1}$H NMR (400 MHz, DMSO-$d_6$/TMS), $\delta$/ppm = 13.456 (s, −O**H**, 1H), 9.078 (d, −C**H**, 1H), 8.797 (dd, −C**H**, 1H), 8.273 (dt, −C**H**, 1H), 7.552 (m, −C**H**, 1H). $^{13}$C NMR (100 MHz, DMSO-$d_6$/TMS), $\delta$/ppm = 166.31 (−**C**OOH), 153.35 (−CH**C**HN−), 150.25 [−N**C**HC(COOH)], 137.00 [−CH**C**H-C(COOH)], 126.57 [−**C**(COOH)], 123.85 (−**C**HCHN−). The observed $^{1}$H and $^{13}$C NMR spectra are in good agreement with those reported in a reference database.[36] No impurities were detected by GC-MS. The absence of water in the sample was corroborated by the lack of the typical H−O−H bending frequency at 1644 cm$^{-1}$ in the DRIFT spectra. DRIFT analysis in KBr also showed no chemical differences between the original material and a sample dried for 24 h at 358 K, as recommended for the use of NIST SRM 2151 in combustion calorimetry.[32]

**Differential Scanning Calorimetry (DSC).** The determination of the temperatures and enthalpies of fusion and solid−solid phase transition by differential scanning calorimetry was made on a DSC 7 from Perkin-Elmer. The experiments were performed at a heating rate of 10 K·min$^{-1}$ in the temperature range 298−523 K. The temperature and heat flow scales of the instrument were previously calibrated at the same heating rate by using indium (Perkin-Elmer; mass fraction 0.99999; $T_{fus}$ =

429.75 K, $\Delta_{fus}h^\circ = 28.45$ J·g$^{-1}$). The nicotinic acid samples, with masses in the range 1.9−7.1 mg, were sealed in air, inside aluminum crucibles, and weighed with a precision of 1 $\mu$g in a Mettler M5 microbalance. Nitrogen (Air Liquide N45), at a flow rate of 0.5 cm$^3$·s$^{-1}$, was used as the purging gas.

A temperature-modulated TA Instruments Inc. 2920 MTDSC apparatus, operated as a conventional DSC, was also used to analyze the sample in a wider temperature range (193−523 K). This analysis was mainly conducted to rule out the presence of a possible glass transition indicating the sample to be partially amorphous. In this case, ~1.9 mg of compound was weighed with a precision of 0.1 $\mu$g in a Mettler UMT2 ultramicrobalance and sealed under air in an aluminum pan. Helium (Air Liquide N55), at a flow rate of 0.5 cm$^3$·s$^{-1}$, was used as the purging gas. The temperature and heat flow scales of the instrument were calibrated as previously described.[37] The heating rate was 10 K·min$^{-1}$.

**Combustion Calorimetry.** The standard massic energy of combustion of nicotinic acid was measured using an isoperibol stirred liquid combustion macrocalorimeter previously described.[38] The general procedure was as follows. A platinum crucible with a mass of ~9.3 g was weighed with a precision of ±0.01 mg in a Mettler AT201 balance. The crucible was loaded with a pellet of nicotinic acid (~0.78−0.93 g) and weighed again. The difference between the two weightings gave the mass of the pellet. The crucible containing the compound was adjusted to the sample holder in the bomb head, and the platinum ignition wire (Johnson Matthey; mass fraction: 0.9995; diameter 0.05 mm) was connected between the two discharge electrodes. A cotton thread fuse of empirical formula $CH_{1.887}O_{0.902}$ was weighed to ±0.1 $\mu$g in a Mettler Toledo UMT2 balance. One end of the fuse was tied to the ignition wire, and the other was brought into contact with the pellet. A volume of 1.0 cm$^3$ of distilled and deionized water from a Millipore system (conductivity, <0.1 $\mu$S·cm$^{-1}$) was added to the bomb body by means of a volumetric pipet. The stainless-steel bomb (Parr 1108) of 340 cm$^3$ internal volume was assembled and purged twice by successively charging it with oxygen at a pressure of 1.01 MPa and venting the overpressure. After purging, the bomb was charged with oxygen at a pressure of 3.04 MPa, and a few minutes were allowed for equilibration before closing the inlet valve. The bomb was placed into the calorimeter proper, which was subsequently filled (on average) with 3751.99 g of distilled water, dispensed from a 4 dm$^3$ round-bottom flask. The mass of water was determined by weighing the flask to ±0.01 g, in a Mettler PM6100 balance, before and after transfer of the content into the calorimeter. The calorimeter proper was closed and placed into the thermostatic jacket, whose temperature was maintained at ~301 K with a precision of $\pm 10^{-4}$ K by means of a Tronac PTC 41 temperature controller. The temperature−time data acquisition was started, and the calorimetric experiment began once the baseline progress ensured that heat transfer between the vessel and the jacket conformed to Newton's law (exponential $T$ vs $t$ variation).[12] The temperature measurements were carried out with a resolution better than $3 \times 10^{-5}$ K, by using a YSI 46047 thermistor of 6.0 kΩ nominal resistance at 298.15 K, connected in a four wire configuration to a Hewlett-Packard HP 34420A digital multimeter. The duration of the fore, main, and after periods was 30 min each. The combustion of the sample was initiated at the end of the fore period by discharge of a 2990 $\mu$F capacitor, from a potential of 40 V, through the platinum wire. The discharge current heated the wire, and when the temperature was increased sufficiently, the thread fuse ignited, and the combustion propagated to the pellet of the compound. The nitric acid formed from combustion of the sample and traces of atmospheric $N_2$ remaining inside the bomb after purging was determined by titrating the final bomb solution with aqueous sodium hydroxide (Merck titrisol, 0.01 mol·dm$^{-3}$), using methyl red as an indicator. No carbon residues, indicating incomplete combustion, were found inside the bomb at the end of the experiments. The energy equivalent of the calorimeter, $\varepsilon^\circ = 18562.59 \pm 1.84$ J·K$^{-1}$, was obtained from the combustion of a benzoic acid sample (BA; NIST SRM 39j), whose massic energy of combustion under the certificate conditions was $\Delta_c u$(BA,cert) = −26434 ± 3 J·g$^{-1}$.

**Enthalpy of Sublimation Measurements.** The enthalpy of sublimation of nicotinic acid was determined from vapor-pressure measurements by the Knudsen effusion method[39−41] and by Calvet microcalorimetry.[42,43]

The Knudsen effusion setup was a modified version of that previously described.[39−41] The main change consisted in the adaptation of a new cylindrical brass block, which can accommodate up to three bronze cells with different holes, to the bottom of the vacuum chamber. The block was surrounded by a tubular furnace whose temperature was controlled to better than ±0.1 K by a Eurotherm 902P thermostatic unit driven by a K type thermocouple embedded in the block. The equilibrium temperature inside each cell was assumed to be identical to the temperature of the brass block. This temperature was measured with a precision of ±0.1 K with a Tecnisis 100 Ω platinum resistance thermometer embedded in the block and connected in a four wire configuration to a Keithley 2000 multimeter. The platinum resistance sensors for temperature measurement and control were calibrated against a standard platinum resistance thermometer, which had been calibrated at an accredited facility in accordance to the International Temperature Scale ITS-90. Each of the three cells was initially charged with ~500 mg of sample, and the corresponding mass loss during a run was determined to ±0.01 mg with a Mettler AT201 balance. The effusion holes were drilled in a $2.090 \times 10^{-5}$ m thick copper foil (Cu 99%, Goodfellow Metals) soldered to the cell lids, and had areas of $2.089 \times 10^{-7}$ m$^2$ (cell 1), $2.640 \times 10^{-7}$ m$^2$ (cell 2), and $4.283 \times 10^{-7}$ m$^2$ (cell 3), respectively. Before insertion into the brass block, the bottom and sides of the Knudsen cells were covered with a thin film of Apiezon N. This ensured a better thermal contact between the cell and the temperature controlled metal block. Evacuation of the system was started after the cells were thermally equilibrated with the block for 45−60 min, under a nitrogen atmosphere. Typically, a pressure of $1 \times 10^{-3}$ Pa was reached in less than 3 min and a final constant pressure of $8 \times 10^{-5}$ Pa was obtained in about 20 min. The experiment was ended by stopping the pumping and filling the vacuum chamber with nitrogen. DRIFT analysis in KBr showed no chemical differences between the original compound and samples collected from the surface and bulk of the material present inside each cell at the end of the measurements (see the Supporting Information). This was also corroborated by the corresponding elemental analysis on the bulk material (average of two determinations): C 58.64%, H 4.04%, N 11.39% (cell 1); C 58.88%, H 4.04%, N 10.92% (cell 2); C 58.41%, H 4.07%, N 11.35% (cell 3).

Two series of Calvet microcalorimetry experiments separated by 1 year were performed. In the first series, the temperature of the calorimeter was set to 376.5 K. A sample with a mass in the range 2.8−11.0 mg was placed into a small glass capillary and weighed with a precision of 1 $\mu$g in a Mettler M5 balance. The capillary was equilibrated for ~15 min at 298 K, inside a

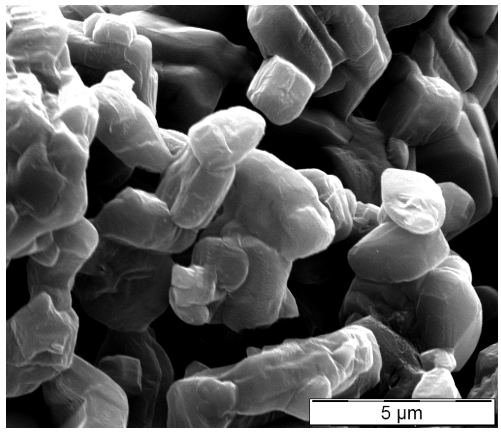


**Figure 1.** SEM micrograph of the nicotinic acid sample (NIST SRM 2151) used in the thermochemical experiments.

furnace positioned above the entrance of the sample cell, and subsequently dropped into the calorimeter under $N_2$ atmosphere. After dropping, an endothermic peak due to the heating of the sample from 298 to 376.5 K was first observed. When the signal returned to the baseline, the sample and reference cells were simultaneously evacuated to 0.13 Pa and the measuring curve associated with the sublimation of the compound was acquired. The corresponding enthalpy of sublimation was subsequently derived from the area of that curve, $A$, the area of the pumping background contribution, $A_b$, and the energy equivalent of the apparatus, $\varepsilon$. The value of $A_b$ was determined from independent runs where only gaseous nitrogen was pumped out of the calorimetric cells and $\varepsilon$ was obtained by electrical calibration.[42] The same procedure was followed in the second series of experiments, which were carried out at 374.8 K and with masses of sample in the range 1.9−5.0 mg. No decomposition or unsublimed residues were found inside the capillaries or calorimetric cell at the end of the experiments. Small residues, which could not be analyzed, were systematically found, however, in two series of measurements performed at 353.7 and 357.6 K, and these were discarded.

**Computational Details.** Density functional theory (DFT),[27] Gaussian-3 theory with second-order Møller−Plesset (G3MP2),[28] and complete basis set - quadratic Becke3 (CBS-QB3)[29,30] procedures were applied to predict thermochemical properties of the systems under examination. In the case of the DFT methods, full geometry optimizations and frequency predictions were carried out with the B3LYP[44,45] hybrid functional using the 6-311++G(d,p),[46,47] cc-pVTZ,[48,49] and aug-cc-pVTZ[49,50] basis sets. The corresponding molecular energies were converted to standard enthalpies at 298.15 K by using zero point energy (ZPE) and thermal energy corrections calculated at the same level of theory. The obtained vibration frequencies and ZPEs were not scaled, unless otherwise stated. The DFT, G3MP2, and CBS-QB3 calculations were performed with the Gaussian-03 package.[51]

## Results and Discussion

**Structure.** The SEM micrograph in Figure 1 shows that from a morphological point of view the sample was composed of smooth-faced prismatic particles. Image analysis carried out on 103 particles using the Olympus Cell$^D$ 2.6 software, led to a Feret's mean diameter (the mean value of the distance between pairs of parallel tangents to the projected outline of the particle, like in a measurement with a caliper)[52] of $d_F = 3.68 \pm 1.38$ $\mu$m and an aspect ratio (the maximum ratio of width and height of a bounding rectangle for the measured object) of $A_r = 1.46 \pm 0.35$. The indicated uncertainties represent standard errors of the mean.

The powder pattern obtained at 298 ± 2 K was indexed as monoclinic, space group $P2_1/c$, with $a = 7.181$ Å, $b = 11.679$ Å, $c = 7.233$ Å, and $\beta = 113.49°$. These results are in excellent agreement with those of previously reported single crystal X-ray diffraction experiments carried out at 293 K: $P2_1/c$, $a = 7.186(2)$ Å, $b = 11.688(3)$ Å, $c = 7.231(2)$ Å, $\beta = 113.55(6)°$.[53,54] The single crystal X-ray diffraction data show that, in this phase, the molecules of nicotinic acid adopt conformation **1**,[53,54] which is predicted by the B3LYP/6-311++G(d,p), B3LYP/cc-pVTZ, B3LYP/aug-cc-pVTZ, G3MP2, and CBS-QB3 calculations carried out in this work to be lower in Gibbs energy by ~1 kJ·mol$^{-1}$ than conformation **2** (see below).

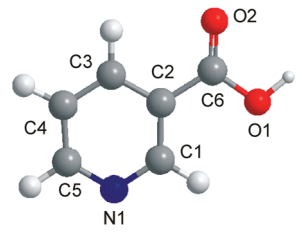


**1**

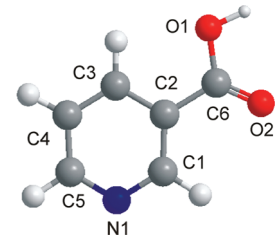


**2**

To the best of our knowledge, the structure of nicotinic acid in the gas phase has not been determined (e.g., from electron diffraction measurements). The bond distances and angles reported for the solid state[53,54] are compared in Table 1 with those predicted for the equivalent configuration of the isolated molecule at the B3LYP/cc-pVTZ level of theory. The calculated data for conformation **2** were also included in the table. It can be concluded from Table 2 that the B3LYP/cc-pVTZ model accurately reproduces most structural features of the nicotinic acid molecule given by the X-ray diffraction analysis. Hence, for example, the differences between the experimental and calculated C−C and N−C bond distances in the pyridine ring are smaller than 0.8%. Not unexpectedly, the largest deviation found ($\Delta = -3.52\%$) refers to the C6−O1 bond, where O1 acts as the donor atom in a O−H···N hydrogen bond in the solid state but not in the gaseous state. A similar conclusion can be drawn if the bond angles are considered: the larger deviations are observed for the angles involving the N1 atom or the COOH group which are implicated in hydrogen bond formation in the solid state. It should also be mentioned that no benefit in terms of the accuracy of the structural predictions was found by the use of the larger aug-cc-pVTZ or 6-311++G(d,p) basis sets (see the Supporting Information).

Packing diagrams of the nicotinic acid form studied in this work, obtained from reported single crystal X-ray diffraction data at 293 K[53,54] by using the Mercury 2.2 program,[55] are illustrated in Figures 2 and 3. As shown in Figure 2, the unit cell contains two antiparallel dimeric units (labeled $A$ and $B$), related by a center of symmetry. These units are arranged in infinite zigzag chains C(6) along the $b$ axis (Figure 3a), sustained by strong O−H···N hydrogen bonds ($d_{OH\cdots N} = 1.843$ Å, $d_{O\cdots N} = 2.660$ Å) and reinforced by weaker C−H···O contacts ($d_{CH\cdots O} = 2.550$ Å). The two layers of chains are situated at a distance of 3.54 Å and do not interact among themselves, except by some possible degree of $\pi-\pi$ stacking along the $c$ axis. They show however C−H···O contacts with adjacent chains situated above and below in approximately parallel planes (Figure 3b).

**TABLE 1: Experimental[a] and Calculated[b] Bond Distances (in Å) and Bond Angles (in Degrees) for Nicotinic Acid**

| | 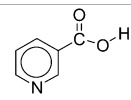 | | | 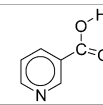 |
|---|---|---|---|---|
| | Experimental (solid) | B3LYP/cc-pVTZ | Δ%[c] | B3LYP/cc-pVTZ |
| Bond distance | | | | |
| C1–N1 | 1.342 | 1.332 | 0.75 | 1.330 |
| C5–N1 | 1.343 | 1.334 | 0.67 | 1.334 |
| C6–O1 | 1.307 | 1.353 | –3.52 | 1.356 |
| C6–O2 | 1.211 | 1.206 | 0.41 | 1.206 |
| C1–C2 | 1.398 | 1.397 | 0.07 | 1.397 |
| C2–C3 | 1.405 | 1.396 | 0.64 | 1.394 |
| C3–C4 | 1.383 | 1.384 | –0.07 | 1.385 |
| C4–C5 | 1.392 | 1.392 | 0.00 | 1.391 |
| C2–C6 | 1.490 | 1.484 | 0.40 | 1.483 |
| Bond angle | | | | |
| C1–N1–C5 | 118.9 | 117.5 | 1.18 | 117.4 |
| C2–C1–N1 | 121.7 | 123.3 | –1.31 | 123.5 |
| C3–C2–C1 | 119.0 | 118.4 | 0.50 | 118.3 |
| C4–C3–C2 | 118.8 | 118.7 | 0.08 | 118.5 |
| C5–C4–C3 | 118.7 | 118.4 | 0.25 | 118.6 |
| N1–C5–C4 | 123.0 | 123.7 | –0.57 | 123.7 |
| C6–C2–C3 | 118.7 | 118.9 | –0.17 | 123.0 |
| C6–C2–C1 | 122.3 | 122.8 | –0.41 | 118.6 |
| O1–C6–C2 | 115.2 | 113.0 | 1.91 | 112.7 |
| O2–C6–C2 | 121.7 | 124.6 | –2.38 | 125.0 |
| O1–C6–O2 | 123.2 | 122.4 | 0.65 | 122.3 |

[a] References 53 and 54. [b] This work, see structures **1** and **2** for labeling schemes. [c] Δ represents the difference between the experimental bond distance or angle and the corresponding value calculated for conformation **1** (that is also adopted in the crystalline state) by the B3LYP/cc-pVTZ method.

**TABLE 2: Results of the Combustion Calorimetric Experiments on Nicotinic Acid**

| | | | | | | |
|---|---|---|---|---|---|---|
| $m$(NA)/g | 0.93275 | 0.89473 | 0.91223 | 0.88510 | 0.84879 | 0.78127 |
| $m$(cotton)/g | 0.0024156 | 0.0023012 | 0.0036117 | 0.0022986 | 0.0019878 | 0.0022186 |
| $\Delta m(H_2O)$/g | 0.15 | 0.28 | 0.18 | −0.54 | 0.17 | 0.43 |
| $10^4 \cdot n(HNO_3)$/mol | 6.69 | 7.06 | 7.84 | 7.07 | 5.67 | 5.86 |
| $\varepsilon_i$/J·K$^{-1}$ | 15.53 | 15.48 | 15.51 | 15.47 | 15.43 | 15.35 |
| $\varepsilon_f$/J·K$^{-1}$ | 15.98 | 15.88 | 15.88 | 15.86 | 15.87 | 15.72 |
| $T_i$/K | 298.1753 | 298.2332 | 298.2228 | 298.2269 | 298.3111 | 298.1821 |
| $T_f$/K | 299.4294 | 299.4306 | 299.4776 | 299.4237 | 299.4821 | 299.2744 |
| $\Delta T_c$/K | 0.1345 | 0.1236 | 0.1585 | 0.1343 | 0.1529 | 0.1547 |
| $\Delta_{ign}U$/J | 0.51 | 0.58 | 0.33 | 0.35 | 0.37 | 0.55 |
| $-\Delta_{IBP}U$/J | 20800.77 | 19950.27 | 20368.10 | 19736.89 | 18915.15 | 17420.17 |
| $\Delta_\Sigma U$/J | 19.25 | 18.36 | 18.73 | 18.14 | 17.38 | 15.86 |
| $\Delta U(HNO_3)$/J | 39.94 | 42.15 | 46.80 | 42.21 | 33.85 | 34.98 |
| $-\Delta U$(cotton)/J | 40.02 | 38.12 | 59.83 | 38.08 | 32.93 | 36.75 |
| $\Delta U$(NA)/J | 20701.56 | 19851.64 | 20242.74 | 19638.46 | 18830.99 | 17332.58 |
| $-\Delta_c u°$(NA, cr)/J·g$^{-1}$ | 22194.11 | 22187.30 | 22190.39 | 22187.84 | 22185.69 | 22185.13 |

These contacts labeled *a* and *b* (for *a*, $d_{CH\cdots O} = 2.576$ Å; for *b*, $d_{CH\cdots O} = 2.608$ Å) together with the analogous interaction that reinforces the C(6) chains (here designated by *c*) are part of three centered bifurcated C−H···O hydrogen bonds involving the carbonyl oxygen of the COOH group as the common acceptor (Figure 3c). As illustrated in Figure 3b, when viewed along the *b* axis, alternate layers of *A* and *B* type chains can be observed. These reflect the 3D propagation of the dimeric motifs found inside the unit cell (Figure 2) throughout the lattice. Two different and short interplanar distances (1.48 and 2.06 Å) can be distinguished in Figure 3b. The longest (2.06 Å) separates a pair of planes containing C(6) chains of the same type (either *AA* or *BB*). The shortest (1.48 Å) corresponds to planes holding chains of different types (*AB*).

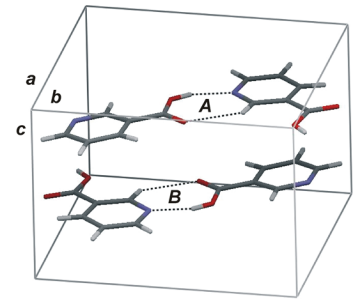


**Figure 2.** Unit cell of the monoclinic (space group $P2_1/c$) nicotinic acid form studied in this work, with indication of the *a*, *b*, and *c* axis. The different orientations of the dimeric units inside the cell are denoted by *A* and *B*, respectively.

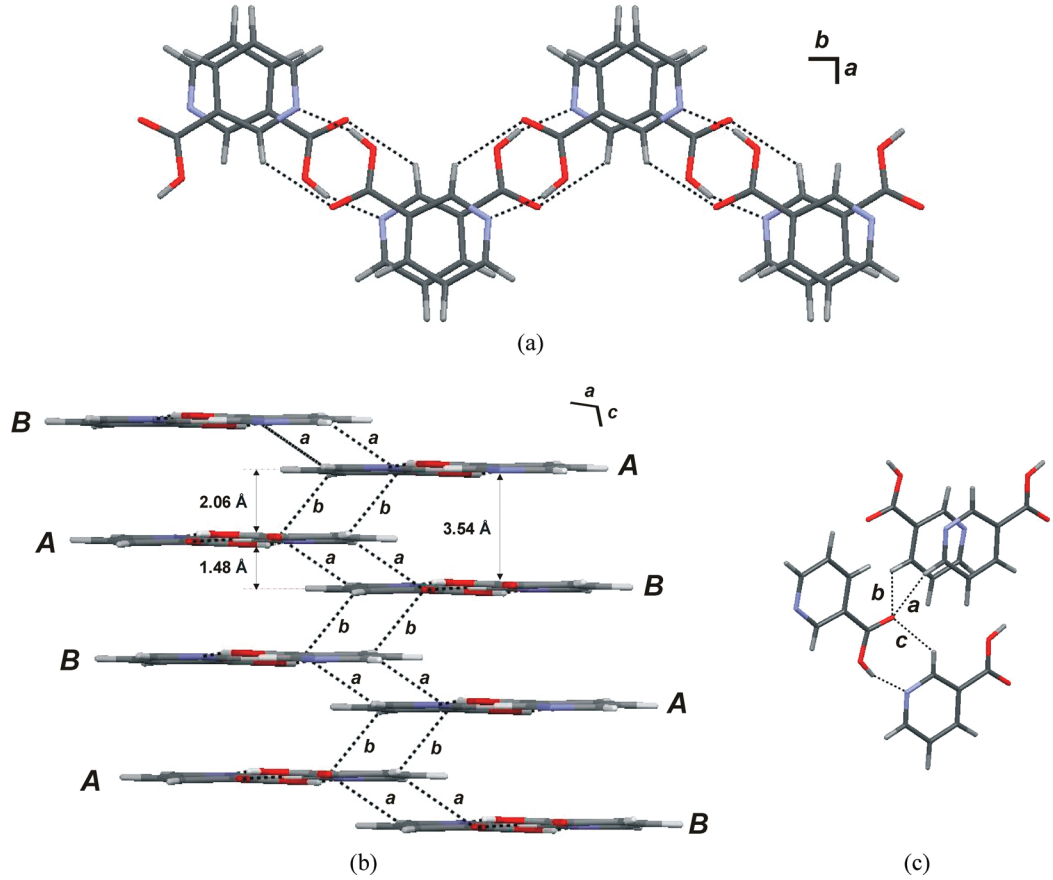


**Figure 3.** (a) Two layers of infinite C(6) chains viewed along the *c* axis. (b) View along the *b* axis, displaying the two types of interchain CH···O contacts $a = 2.576$ Å and $b = 2.608$ Å and the distances between planes containing chains with *A* or *B* type sequences of nicotinic acid molecules as defined in Figure 2. (c) Three centered bifurcated C−H···O hydrogen bond motif that sustains the interactions between chains in adjacent planes and reinforces the O−H···N hydrogen bond within a chain.

**Energetics.** The 2005 IUPAC recommended standard atomic masses were used in the calculation of all molar quantities.[56]

The onset ($T_{on}$) and maximum ($T_{max}$) temperatures of the fusion peak obtained by DSC were $T_{on} = 507.3 \pm 1.4$ K and $T_{max} = 509.9 \pm 0.8$ K, respectively, and the corresponding enthalpy of fusion, $\Delta_{fus}H_m = 27.8 \pm 0.2$ kJ·mol$^{-1}$. Fusion was preceded by a reversible phase transition for which $T_{on} = 452.9 \pm 0.5$ K, $T_{max} = 456.1 \pm 0.4$ K, and $\Delta_{trs}H_m = 0.83 \pm 0.10$ kJ·mol$^{-1}$. The uncertainties indicated for $T_{on}$, $T_{max}$, $\Delta_{trs}H_m$, and $\Delta_{fus}H_m$ correspond to twice the standard error of the mean of seven determinations. The values of $T_{on}$ and $T_{max}$ corresponding to the fusion event observed in this work are within the interval 508.7−509.8 K attributed to pure nicotinic acid in a comprehensive study of its temperature of fusion.[57] The corresponding $\Delta_{fus}H_m = 27.8 \pm 0.2$ kJ·mol$^{-1}$ also ranks among the highest values published for the enthalpy of fusion of nicotinic acid.[21,58−61] This indicates the sample to be significantly crystalline, in agreement with the X-ray powder diffraction and SEM evidence, and also with the fact that no glass transition was detected in a DSC analysis carried out in the range 193−523 K at a heating rate of 10 K·min$^{-1}$. It should be noted that the reported temperatures and enthalpies of fusion of nicotinic acid vary in a considerably wide range: $T_{fus} = 507.0 \pm 0.8$,[59] 509.1,[60] 509.16 ± 0.01,[21] 509.2 ± 0.6,[57] 509.5 ± 0.5,[62] 509.8 ± 0.7,[59] 510,[61,63] 512.0,[18] and 515.5 K;[64] $\Delta_{fus}H_m = 12.4$,[58] 13.01 ± 0.32,[21] 20.8 ± 0.4,[59] 24.6,[58] 26.7 ± 0.4,[59] 27.57,[60] and 30 kJ·mol$^{-1}$.[61] The same applies to the phase transition: $T_{trs} = 451.4$,[60] 452.0 ± 0.6,[59] 453.2 ± 0.5,[59] 457,[63,64] and 457.7 K;[18] $\Delta_{trs}H_m = 0.78 \pm 0.01$,[59] 0.52 ± 0.01,[59] and 0.81 kJ·mol$^{-1}$.[60] This probably reflects the fact that they seem to be notably influenced by the crystallinity and particle size of the sample. For example, in differential thermal analysis experiments carried out at 5 K·min$^{-1}$, Moussaoui et al.[59] observed that grinding a sample of nicotinic acid led to decreases of ∼3 K and ∼6 kJ·mol$^{-1}$ in $T_{fus}$ and $\Delta_{fus}H_m$, respectively. In the same experiments, $T_{trs}$ increased by 1.2 K and $\Delta_{trs}H_m$ decreased by 0.26 kJ·mol$^{-1}$. Furthermore, DSC runs carried out at 10 K·min$^{-1}$ by Rehman et al.[58] showed that an improvement of the crystallinity of the sample could translate into a change of $\Delta_{fus}H_m$ from ∼12 to ∼25 kJ·mol$^{-1}$.

The results of the combustion calorimetric experiments are given in Table 2, where *m*(NA) and *m*(cotton) are the masses of nicotinic acid and cotton thread fuse, respectively; $\Delta m(H_2O)$ is the difference between the mass of water inside the calorimeter proper during the main experiment and that used on average in the calibration (3751.99 g); $n(HNO_3)$ is the amount of substance of nitric acid formed in the bomb process; $\varepsilon_i$ and $\varepsilon_f$ are the energy equivalents of the bomb contents in the initial and final states of the bomb process, respectively; $T_i$ and $T_f$ represent the initial and final temperatures of the experiment; $\Delta T_c$ is the contribution to the observed temperature rise of the calorimeter proper due to the heat exchanged with the surroundings and the heat dissipated by the temperature sensor; $\Delta_{ign}U$ is the electrical energy supplied for ignition of the sample, which was calculated from

$$\Delta_{ign}U = \frac{(V_i^2 - V_f^2)C}{2} \quad (1)$$

where $V_i$ and $V_f$ are the potential of the condenser of capacitance $C = 2990\ \mu F$ before and after its discharge through the platinum ignition wire, respectively; $\Delta_{IBP}U$ is the internal energy change associated with the bomb process under isothermal conditions, at 298.15 K; $\Delta_\Sigma U$ represents the sum of all corrections necessary to reduce $\Delta_{IBP}U$ to the standard state (Washburn corrections), which were derived as recommended for organic compounds containing C, H, O, and N,[12,65,66] by using the following heat capacity, density, and $-(\partial u/\partial p)_T$ data for crystalline nicotinic acid: $c_p^\circ = 1.21\ J\cdot g^{-1}$,[60] $\rho = 1.469\ g\cdot cm^{-3}$,[53] $-(\partial u/\partial p)_T = 6.91 \times 10^{-8}\ J\cdot g^{-1}\ Pa^{-1}$;[67] $\Delta U(HNO_3)$ is the energy change associated with the formation of nitric acid which was based on $-59.7\ kJ\cdot mol^{-1}$ for the molar internal energy of formation of $HNO_3$(aq) of concentration 0.1 $mol\cdot dm^{-3}$ from $^5/_4O_2$(g), $^1/_2N_2$(g), and $^1/_2H_2O$ (l);[68] $\Delta U$(cotton) is the energy associated with the combustion of the cotton fuse of standard specific energy of combustion $\Delta_c u^\circ(\text{cotton}) = -16565.9 \pm 8.6\ J\cdot g^{-1}$;[38] $\Delta U$(NA) is the contribution of nicotinic acid for the energy of the isothermal bomb process; and, finally, $\Delta_c u^\circ$(NA, cr) is the corresponding standard specific internal energy of combustion.

The values of $T_i$, $T_f$, and $\Delta T_c$ were calculated by using a computer program based on the Regnault−Pfaundler method,[12,69] and $\Delta_{IBP}U$ was derived from[12]

$$\Delta_{IBP}U = [\varepsilon^\circ + \Delta m(H_2O)c_p^\circ(H_2O, l)](T_i - T_f + \Delta T_c) + \varepsilon_i(T_i - 298.15) + \varepsilon_f(298.15 - T_f + \Delta T_c) + \Delta_{ign}U \quad (2)$$

where $c_p^\circ(H_2O, l) = 4.179\ J\cdot g^{-1}$.[68]

The standard specific energies of combustion of nicotinic acid in Table 2 refer to the reaction

$$C_6H_5O_2N(cr) + {}^{25}/_4O_2(g) = 6CO_2(g) + {}^5/_2H_2O(l) + {}^1/_2N_2(g) \quad (3)$$

and were obtained from

$$\Delta_c u^\circ(NA, cr) = \frac{1}{m(NA)}[\Delta_{IBP}U + \Delta_\Sigma U - \Delta U(HNO_3) - \Delta U(\text{cotton})] \quad (4)$$

They lead to the mean value $\Delta_c u^\circ(NA, cr) = -22188.41 \pm 1.37\ J\cdot g^{-1}$, at 298.15 K, from which $\Delta_c U_m^\circ(NA, cr) = -2731.60 \pm 0.88\ kJ\cdot mol^{-1}$ and $\Delta_c H_m^\circ(NA, cr) = -2730.98 \pm 0.88\ kJ\cdot mol^{-1}$ can be derived. The uncertainties indicated for $\Delta_c u^\circ$(NA, cr) represent the standard error of the mean of the six individual measurements, and those of $\Delta_c U_m^\circ$(NA, cr) and $\Delta_c H_m^\circ$(NA, cr) correspond to twice the overall standard error of the mean, including the contributions from the calibration with benzoic acid.[70] From the value of $\Delta_c H_m^\circ$(NA, cr) indicated above, $\Delta_f H_m^\circ(CO_2, g) = -393.51 \pm 0.13\ kJ\cdot mol^{-1}$,[71] and $\Delta_f H_m^\circ(H_2O, l) = -285.830 \pm 0.042\ kJ\cdot mol^{-1}$,[71] it is possible to conclude that $\Delta_f H_m^\circ(NA, cr) = -344.7 \pm 1.2\ kJ\cdot mol^{-1}$.

The enthalpy of sublimation of nicotinic acid was obtained from vapor-pressure vs temperature measurements by the Knudsen effusion method and also by drop-sublimation Calvet microcalorimetry (detailed results are given as Supporting Information). In the Knudsen effusion experiments, the values of $p$ were calculated from[72,73]

$$p = \frac{m}{At}\left(\frac{2\pi RT}{M}\right)^{1/2}\left(\frac{8r + 3l}{8r}\right)\left(\frac{2\lambda}{2\lambda + 0.48r}\right) \quad (5)$$

where $m$ is the mass loss during the time $t$; $A$, $l$, and $r$ are the area, the thickness, and the radius of the effusion hole, respectively; $M$ is the molar mass of the compound under study, $R = 8.314472\ J\cdot K^{-1}\cdot mol^{-1}$ is the gas constant, $T$ is the absolute temperature, and $\lambda$ is the mean free path given by[74]

$$\lambda = \frac{kT}{\sqrt{2}\pi\sigma^2 p} \quad (6)$$

Here, $k$ represents the Boltzmann constant and $\sigma$ the collision diameter. The collision diameter of nicotinic acid was estimated as 585 pm from the van der Waals volume of the molecule calculated with the GEPOL93 program,[75] based on the molecular structure reported by Kutoglu and Scheringer.[53] The van der Waals radii of carbon (170 pm), hydrogen (120 pm), nitrogen (155 pm), and oxygen (152 pm) given by Bondi were selected for this calculation.[76] Since the mean free path in eq 6 is pressure dependent, an iterative method was needed to obtain the vapor pressure of the compound through eqs 5 and 6. As a first approximation, $p$ was calculated by ignoring the $\lambda$ dependent term in eq 5. The obtained result was subsequently used to derive $\lambda$ from eq 6. The calculated mean free path was introduced in eq 5, and a second $p$ value was calculated. The iteration was continued until the difference between successive values of $p$ was smaller than $10^{-8}$ Pa. The vapor pressure against temperature data were fitted to eq 7 (Figure 4):[77]

$$\ln p = a - \frac{b}{T} \quad (7)$$

where the slope $b$ is related to the enthalpy of sublimation at the average of the highest and lowest temperatures of the range covered in each series of experiments, $T_m$, by $\Delta_{sub}H_m^\circ(NA, T_m) = bR$. The obtained results, which refer to $T_m = 366.5$ K, were the following: for cell 1, $a = 35.43 \pm 0.72$, $b = 13152.4 \pm 264.2$, and $\Delta_{sub}H_m^\circ(NA, 366.5\ K) = 109.4 \pm 4.6\ kJ\cdot mol^{-1}$; for cell 2, $a = 35.74 \pm 0.63$, $b = 13295.8 \pm 229.2$, and $\Delta_{sub}H_m^\circ(NA, 366.5\ K) = 110.6 \pm 3.9\ kJ\cdot mol^{-1}$; for cell 3, $a = 34.88 \pm 0.59$, $b = 12982.2 \pm 214.7$, and $\Delta_{sub}H_m^\circ(NA, 366.5\ K) = 107.9 \pm 3.7\ kJ\cdot mol^{-1}$. The uncertainties assigned to $a$ and $b$ are the corresponding standard errors, and that for $\Delta_{sub}H_m^\circ(NA, 366.5\ K)$ includes Student's factor for 95% confidence level[78] (cell 1, $t = 2.093$ for 20 independent measurements; cells 2 and 3, $t = 2.064$ for 25 independent measurements). Correction of the

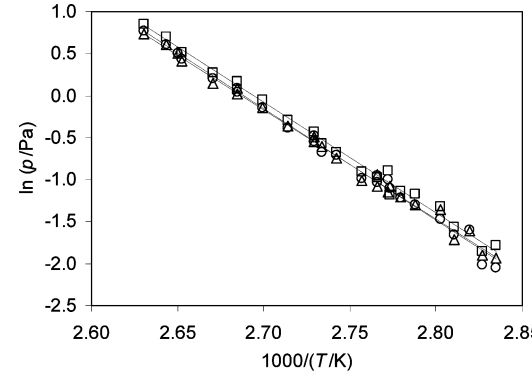


**Figure 4.** Vapor pressure of nicotinic acid as a function of the temperature: (□) cell 1 ($A = 2.089 \times 10^{-7}$ m$^2$, $r = 2.579 \times 10^{-4}$ m, $l = 2.09 \times 10^{-5}$ m); (○) cell 2 ($A = 2.640 \times 10^{-7}$ m$^2$, $r = 2.899 \times 10^{-4}$ m, $l = 2.09 \times 10^{-5}$ m); (△) cell 3 ($A = 4.283 \times 10^{-7}$ m$^2$, $r = 3.692 \times 10^{-4}$ m, $l = 2.09 \times 10^{-5}$ m).

**TABLE 3: Standard Molar Enthalpies of Combustion, Formation, and Sublimation of Nicotinic Acid at 298.15 K (Data in kJ·mol$^{-1}$)**

| $-\Delta_c H^\circ_m$(NA, cr) | $-\Delta_f H^\circ_m$(NA, cr) | $\Delta_{sub} H^\circ_m$(NA) | $-\Delta_f H^\circ_m$(NA, g) |
|---|---|---|---|
| 2730.98 ± 0.88[a] | 344.7 ± 1.2[a] | 112.1 ± 0.5[a] | 232.6 ± 1.3 |
| 2730.63 ± 0.69[b] | 345.0 ± 1.1[b] | | |
| 2730.81 ± 0.76[c] | 344.8 ± 1.1[c] | | |
| 2731.10 ± 2.19[d] | 344.5 ± 2.3[d] | 103.8 ± 1.2[d] | 240.7 ± 2.6 |
| | | 123.4 ± 1.2[e] | |
| | | 124.4 ± 0.6[f] | |
| | | 117.4 ± 0.9[g] | |

[a] This work. [b] Reference 67. [c] Reference 24. [d] Reference 21. [e] Reference 19. [f] Reference 20; weighted mean of five independent determinations (see text). [g] Reference 22; this value refers to a high temperature nicotinic acid phase (see text).

obtained $\Delta_{sub} H^\circ_m$(NA, 366.5 K) values to 298.15 K led to $\Delta_{sub} H^\circ_m$(NA) = 112.4 ± 4.6 kJ·mol$^{-1}$ (cell 1), $\Delta_{sub} H^\circ_m$(NA) = 113.6 ± 3.9 kJ·mol$^{-1}$ (cell 2), and $\Delta_{sub} H^\circ_m$(NA) = 110.9 ± 3.7 kJ·mol$^{-1}$ (cell 3). The correction was made through the equation

$$\Delta_{sub} H^\circ_m(\text{NA, 298.15 K}) = \Delta_{sub} H^\circ_m(\text{NA}, T) + \int_T^{298.15\,\text{K}} [C^\circ_{p,m}(\text{NA, g}) - C^\circ_{p,m}(\text{NA, cr})]\, dT \quad (8)$$

where $C^\circ_{p,m}$(NA, cr) and $C^\circ_{p,m}$(NA, g) are the standard molar heat capacities of the compound in the crystalline and gaseous states, respectively. For the crystalline state, the calculations were based on the equation[60]

$$C^\circ_{p,m}(\text{NA, cr})/\text{J·K}^{-1}\text{·mol}^{-1} = 115.77043 + 59.91381x + 7.53269x^2 + 1.2433x^3 - 2.39857x^4 + 7.21254x^5 + 4.134x^6 \quad (9)$$

where $x = (T - 223.5)/144.5$ and $T$ is the absolute temperature. Equation 9 is valid in the temperature range 79−368 K. The heat capacity of gaseous nicotinic acid was taken as

$$C^\circ_{p,m}(\text{NA, g})/\text{J·K}^{-1}\text{·mol}^{-1} = 6.28434 + 0.385604T - 8.53356 \times 10^{-5}T^2 \quad (10)$$

Equation 10 originated from a least-squares fitting to the $C^\circ_{p,m}$(NA, g) data calculated by statistical mechanics,[79] using vibration frequencies obtained by the B3LYP/cc-pVTZ method and scaled by 0.965.[80]

The first and second series of drop-sublimation Calvet microcalorimetry experiments led to $\Delta_{sub} H^\circ_m$(NA, 376.5 K) = 108.79 ± 0.93 kJ·mol$^{-1}$ and $\Delta_{sub} H^\circ_m$(NA, 374.8 K) = 108.43 ± 0.64 kJ·mol$^{-1}$, respectively, where the uncertainty quoted represents twice the overall standard error of five independent results including the contribution from the electrical calibration. Correction of these values to 298.15 K, using eqs 8−10, leads to $\Delta_{sub} H^\circ_m$(NA) = 112.4 ± 0.9 kJ·mol$^{-1}$ and $\Delta_{sub} H^\circ_m$(NA) = 111.9 ± 0.6 kJ·mol$^{-1}$ in good agreement with the corresponding values obtained by the Knudsen effusion method. The weighted mean[70] of the five results from both techniques, at 298.15 K, $\Delta_{sub} H^\circ_m$(NA) = 112.1 ± 0.5 kJ·mol$^{-1}$, was selected in this work.

The values of $\Delta_c H^\circ_m$(NA, cr), $\Delta_f H^\circ_m$(NA, cr), and $\Delta_{sub} H^\circ_m$(NA) here determined are compared in Table 3 with those recalculated, when possible, from published results by using identical auxiliary data (e.g., molar mass, heat capacity).[19−21,24,67] Also indicated in Table 3 are the standard molar enthalpies of formation of gaseous nicotinic acid, $\Delta_f H^\circ_m$(NA, g), calculated from the corresponding $\Delta_f H^\circ_m$(NA, cr) and $\Delta_{sub} H^\circ_m$(NA). It can be concluded from Table 3 that the enthalpy of formation of nicotinic acid in the crystalline state obtained in this work is in excellent agreement with all of the previously reported values.

**TABLE 4: Experimental and Theoretical Enthalpies of Reaction 11**

| | $-\Delta_r H^\circ_m(11)$/kJ·mol$^{-1}$ |
|---|---|
| B3LYP/cc-pVTZ | 3.6 |
| B3LYP/aug-cc-pVTZ | 3.7 |
| B3LYP/6-311++G(d,p) | 4.2 |
| G3MP2 | 4.3 |
| CBS-QB3 | 4.0 |
| experimental | 3.6 ± 2.7 |

To the best of our knowledge, four determinations of the enthalpy of sublimation of nicotinic acid appeared in the literature up to now. Drop-sublimation Calvet microcalorimetry experiments carried out by Bickerton et al.,[19] at 420 K, led to $\Delta_{sub} H^\circ_m$(NA) = 123.4 ± 1.2 kJ·mol$^{-1}$ at 298.15 K. This value diverges by +11.3 kJ·mol$^{-1}$ from that obtained in this work. No reassessment based on the same auxiliary data used here was possible, since the primary data corresponding to 420 K were not published. The results of Calvet microcalorimetry measurements performed by Sabbah and Ider[21] on a sample subliming from a Knudsen cell at 362.2 K give $\Delta_{sub} H^\circ_m$(NA, 362.2 K) = 101.1 ± 1.2 kJ·mol$^{-1}$, where the indicated uncertainty corresponds to twice the standard error of seven independent results. Correction of this value to 298.15 K through eqs 8−10 leads to $\Delta_{sub} H^\circ_m$(NA) = 103.8 ± 1.2 kJ·mol$^{-1}$, which differs by −8.3 kJ·mol$^{-1}$ from the result recommended in this work. From the five independent experiments carried out by Ribeiro da Silva et al.[20] using the Knudsen effusion method coupled with quartz crystal balance detection, it is possible to derive $\Delta_{sub} H^\circ_m$(NA) = 126.2 ± 1.6 kJ·mol$^{-1}$ at 351.6 K, 116.3 ± 3.5 kJ·mol$^{-1}$ at 353.8 K, 117.8 ± 4.8 kJ·mol$^{-1}$ at 355.8 K, 123.8 ± 1.6 kJ·mol$^{-1}$ at 358.2 K, and 120.9 ± 0.7 kJ·mol$^{-1}$ at 360.6 K. The indicated uncertainties are those reported by the authors. The corresponding values at 298.15 K, calculated through eqs 8−10, are 128.4 ± 1.6, 118.6 ± 3.5, 120.2 ± 4.8, 126.3 ± 1.6, and 123.6 ± 0.7 kJ·mol$^{-1}$. These lead to a weighted mean $\Delta_{sub} H^\circ_m$(NA) = 124.4 ± 0.6 kJ·mol$^{-1}$, which differs by +12.3 kJ·mol$^{-1}$ from the value recommended in this work. Finally, Menon et al.[22] used "Langmuir's" equation to obtain the vapor pressure of nicotinic acid in the range 473.15−483.15 K from thermogravimetry measurements. Three methods of analysis were used. A least-squares fit to the results of the apparently more reliable comparative method led to $\Delta_{sub} H^\circ_m$(NA, 478.2 K) = 99.1 ± 0.9 kJ·mol$^{-1}$. The reference temperature corresponds to the mean value of the interval covered in the experiments, and the assigned uncertainty is the standard error of the slope $b$ of eq 7 multiplied by Student's factor for 95% confidence level ($t$ = 2.228 for 11 independent measurements).[78] Conversion of $\Delta_{sub} H^\circ_m$(NA, 478.2 K) to 298.15 K, using eqs 8−10, yields $\Delta_{sub} H^\circ_m$(NA) = 117.4 ± 0.9 kJ·mol$^{-1}$. It should be noted that this value refers to experiments carried out in a temperature range significantly above the onset of the solid−solid phase transition observed for nicotinic acid by DSC ($T_{on}$ = 452.9 ± 0.5 K, see above). It is, therefore, not strictly comparable to all the other standard molar enthalpies of sublimation in Table 3, since it probably corresponds to a different nicotinic acid solid phase.

The nature of the discrepancies between the $\Delta_{sub}H^{\circ}_{m}$(NA) value recommended here and those obtained from published data (all originating from very credible thermochemistry laboratories) eluded a clear-cut identification. For example, in none of the published work was the crystallinity and phase purity of the samples analyzed by X-ray powder diffraction. Nevertheless, the enthalpy of the only solid−solid phase transition reported for nicotinic acid up to now amounts to less than 1 kJ·mol$^{-1}$ (see above) and it seems, therefore, unlikely that differences in phase purity would translate into changes of up to 12 kJ·mol$^{-1}$ in $\Delta_{sub}H^{\circ}_{m}$(NA). These could, in principle, be traced back to the crystallinity of the samples. Indeed, as mentioned above, a decrease in the crystallinity of solid nicotinic acid was found by Rehman et al.[58] to lower the corresponding enthalpy of fusion by up to 13 kJ·mol$^{-1}$ and a similar effect should be expected for $\Delta_{sub}H^{\circ}_{m}$(NA). In line with this reasoning, the enthalpies of fusion (13.01 ± 0.32 kJ·mol$^{-1}$) and sublimation (103.8 ± 1.2 kJ·mol$^{-1}$) of nicotinic acid reported by Sabbah and Ider[21] are both considerably smaller than the corresponding values recommended in this work (Table 3), thus suggesting that they refer to a material of substantial amorphous character. However, this should also lead to a less negative standard molar enthalpy of formation in the crystalline state and, as shown in Table 3, the $\Delta_{f}H^{\circ}_{m}$(NA, cr) value reported by Sabbah and Ider is in good agreement with all of the other determinations. A similar discussion could not be transposed to the higher $\Delta_{sub}H^{\circ}_{m}$(NA) values of Bickerton et al.[19] and Ribeiro da Silva et al.[20] (Table 3), since, in these cases, the enthalpies of fusion and combustion of the samples used in the sublimation experiments were not reported. To help in the assessment of the internal consistency of our data, we therefore resorted to an isodesmic reaction scheme and to computational chemistry.

The values of $\Delta_{f}H^{\circ}_{m}$(NA, cr) and $\Delta_{sub}H^{\circ}_{m}$(NA) recommended in this work (Table 3) lead to $\Delta_{f}H^{\circ}_{m}$(NA, g) = −232.6 ± 1.3 kJ·mol$^{-1}$, which together with $\Delta_{f}H^{\circ}_{m}$($C_6H_6$, g) = 82.6 ± 0.7 kJ·mol$^{-1}$,[81] $\Delta_{f}H^{\circ}_{m}$($C_5H_5N$, g) = 140.4 ± 0.7 kJ·mol$^{-1}$,[81] and $\Delta_{f}H^{\circ}_{m}$($C_6H_5COOH$, g) = −294.0 ± 2.2 kJ·mol$^{-1}$ [81] allows the calculation of the enthalpy of the isodesmic reaction 11 as $\Delta_{r}H^{\circ}_{m}(11) = -3.6 \pm 2.7$ kJ·mol$^{-1}$.

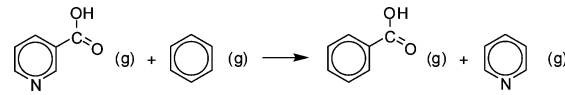


(11)

This value is compared in Table 4 with the corresponding predictions by various theoretical models, which were computed from the data in Table 5. It should be noted that the standard

**TABLE 5: Electronic Energies ($E_{el}$), Zero Point Energies (ZPE), Thermal Corrections ($E_v + E_r + E_t$), Standard Enthalpies ($H^{\circ}$),[a] Standard Gibbs Energies ($G^{\circ}$), and Boltzmann Weights ($p_i$),[b] at 298.15 K, Calculated with the B3LYP/cc-pVTZ, B3LYP/aug-cc-pVTZ, B3LYP/6-311++G(d,p), G3MP2, and CBS-QB3 Methods (Data in Hartree)[c]**

| | | B3LYP/ cc-pVTZ | B3LYP/ aug-cc-pVTZ | B3LYP/ 6-311++G(d,p) | G3MP2 | CBS-QB3 |
|---|---|---|---|---|---|---|
| Nicotinic Acid | $E_{el}$ | −437.021778 | −437.028135 | −436.986711 | −436.337538 | −436.298365 |
| 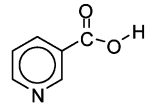 | *ZPE* | 0.103641 | 0.103518 | 0.103264 | 0.100311 | 0.102567 |
| | $E_v+E_r+E_t$ | 0.007017 | 0.007027 | 0.007076 | 0.007170 | 0.007064 |
| | $H^{o}$ | −436.910176 | −436.916646 | −436.875427 | −436.229113 | −436.187790 |
| (Conformation 1) | $G^{o}$ | −436.950184 | −436.956698 | −436.915565 | −436.269320 | −436.227813 |
| | $p_1$ | 0.51 | 0.51 | 0.51 | 0.51 | 0.51 |
| 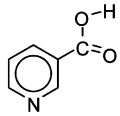 | $E_{el}$ | −437.021345 | −437.027685 | −436.986303 | −436.337107 | −436.297919 |
| | *ZPE* | 0.103618 | 0.103499 | 0.103238 | 0.100299 | 0.102559 |
| | $E_v+E_r+E_t$ | 0.007020 | 0.007033 | 0.0070796 | 0.007171 | 0.007067 |
| | $H^{o}$(298.15 K) | −436.909763 | −436.916209 | −436.875042 | −436.228693 | −436.187349 |
| (Conformation 2) | $G^{o}$(298.15 K) | −436.949792 | −436.956302 | −436.915195 | −436.268915 | −436.227397 |
| | $p_2$ | 0.49 | 0.49 | 0.49 | 0.49 | 0.49 |
| Benzene | $E_{el}$ | −232.333366 | −232.335568 | −232.311301 | −231.925889 | −231.888874 |
|  | *ZPE* | 0.100379 | 0.100320 | 0.100057 | 0.096136 | 0.099135 |
| | $E_v+E_r+E_t$ | 0.004381 | 0.004384 | 0.004407 | 0.004505 | 0.004432 |
| | $H^{o}$(298.15 K) | −232.227662 | −232.229920 | −232.205893 | −231.824304 | −231.784363 |
| Benzoic Acid | $E_{el}$ | −420.983204 | −420.988756 | −420.948272 | −420.312095 | −420.270126 |
| 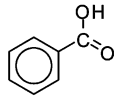 | *ZPE* | 0.115538 | 0.115381 | 0.115149 | 0.111313 | 0.114273 |
| | $E_v+E_r+E_t$ | 0.007104 | 0.007117 | 0.007146 | 0.007297 | 0.007160 |
| | $H^{o}$(298.15 K) | −420.859618 | −420.865314 | −420.825033 | −420.192541 | −420.147749 |
| Pyridine | $E_{el}$ | −248.373203 | −248.376258 | −248.351266 | −247.952827 | −247.918538 |
|  | *ZPE* | 0.088620 | 0.088600 | 0.088343 | 0.085222 | 0.087556 |
| | $E_v+E_r+E_t$ | 0.004265 | 0.004267 | 0.004291 | 0.004362 | 0.004309 |
| | $H^{o}$(298.15 K) | −248.279374 | −248.282447 | −248.257688 | −247.862299 | −247.825729 |

[a] $H^{\circ}(298.15\text{ K}) = E_{el} + \text{ZPE} + E_v + E_r + E_t + RT$, where $E_v$, $E_r$, and $E_t$ represent the vibrational, rotational, and translational contributions. [b] Calculated from eqs 12 or 13 (see text). [c] 1 hartree = 2625.499963 kJ·mol$^{-1}$.

molar enthalpy of nicotinic acid used in the theoretical calculations of $\Delta_r H^\circ_m(11)$ includes contributions from the conformations **1** and **2** mentioned above (e.g., Table 5). The corresponding weights, $p_1$ and $p_2$, respectively, were obtained from

$$p_1 = \frac{1}{1 + e^{-\Delta G^\circ_2/RT}} \quad (12)$$

$$p_2 = 1 - p_1 \quad (13)$$

by assuming that the two conformations were in equilibrium and that this equilibrium was governed by Boltzmann's distribution. In eq 12, $T$ is the absolute temperature, $R$ is the gas constant, and $\Delta G^\circ_2$ represents the difference in Gibbs energy between conformation **2** (highest $G^\circ$) and conformation **1** (lowest $G^\circ$).

As shown in Table 4, the experimentally and theoretically obtained $\Delta_r H^\circ_m(11)$ results are all in excellent agreement. This supports the reliability of the standard molar enthalpies of formation and sublimation of nicotinic acid recommended in this work (Table 3) and indicates a very good thermodynamic consistency with the other experimental data used in the calculation of $\Delta_r H^\circ_m(11)$. Hence, the $\Delta_f H^\circ_m$(NA, cr), $\Delta_{sub} H^\circ_m$(NA), and $\Delta_f H^\circ_m$(NA, g) values here reported can be used as reliable anchor points for discussing the energetics of nicotinic acid.

It should finally be emphasized that the energetics of crystalline materials is sensitive to a multitude of structural effects that are normally difficult to control in practice and can significantly influence the outcome of the measurements when high accuracy and precision are aimed. Thus, for example, the results of calorimetric experiments or vapor pressure determinations may be influenced by the possible existence of different crystalline forms (polymorphs) or amorphous domains coexisting under the same temperature and pressure conditions. Techniques such as X-ray diffraction and DSC are very helpful in signaling the presence of mixtures of polymorphs and amorphous phases and should not be left out of the sample characterization process. An additional concern is lattice imperfections (e.g., vacancies, screw dislocations), which can develop during crystallization and may change in nature and number, as a result of the stresses and strains typical of processing operations, such as drying, grinding, compression, or temperature annealing. In some cases, the measurement of specific properties appears to be more sensitive to sample variability than others. This seems to occur for nicotinic acid where the reported standard molar enthalpies of sublimation show a far larger discrepancy than the corresponding enthalpies of formation in the crystalline state (Table 3). The reproducibility of the solid state is therefore an important issue when accurate data are sought, and the availability of well characterized materials that can be used as references for intercomparison studies necessary. Last but not the least, the discrepancies in $\Delta_f H^\circ_m$(cr) and $\Delta_{sub} H^\circ_m$ ultimately affect the determination of $\Delta_f H^\circ_m$(g), which is frequently used to discuss bonding energetics and to assess the predictions of empirical estimation schemes or computational chemistry methods. In this case, the effect of sample variability may be mitigated if the same material is used to obtain both $\Delta_f H^\circ_m$(cr) and $\Delta_{sub} H^\circ_m$.

**Acknowledgment.** This work was supported by Fundação para a Ciência e a Tecnologia, Portugal (Project PTDC/QUI-QUI/098216/2008). Ph.D. and Post Doctoral grants from FCT are gratefully acknowledged by E.M.G. (SFRH/BD/28458/2006) and C.E.S.B. (SFRH/BPD/43346/2008). Thanks are also due to Nuno Neng at the laboratory of Dr. José M. Nogueira (FCUL, Portugal) for the performance of the GC-MS analysis, to Janine Schwiertz at the group of Prof. Matthias Epple (University of Duisburg-Essen, Germany) for the recording of the SEM images, to Prof. Maria das Dores Ribeiro da Silva (FCUP, Portugal) for helpful comments, and to Prof. Zhi-Cheng Tan (Dalian Institute of Chemical Physics, China) for kindly providing unpublished details about the determination of the enthalpy of formation of nicotinic acid included in Reference 25.

**Supporting Information Available:** Figure S1 with the results of the GC-MS analysis of the nicotinic acid sample used in this work; Figures S2 and S3 with the $^1$H and $^{13}$C NMR spectra, respectively; Table S1 with the details of the powder X-ray diffraction characterization; Tables S2 and S3 with the bond distances and bond angles for conformations **1** and **2** of nicotinic acid calculated at the B3LYP/6-311++G(d,p) and B3LYP/aug-cc-pVTZ levels of theory; Table S4 containing the experimental vapor pressures of nicotinic acid obtained by the Knudsen effusion method; Figures S4−S6 and Table S5 with the results of the DRIFT analysis carried out on the nicotinic acid sample, before and after the Knudsen effusion experiments; Tables S6 and S7 with the details of the drop-sublimation Calvet microcalorimetry experiments. This material is available free of charge via the Internet at http://pubs.acs.org.

## References and Notes

(1) Elvehjem, C. A.; Teply, L. J. *Chem. Rev.* **1943**, *33*, 185–208.
(2) Blum, R. Vitamins. In *Ullmann's Encyclopedia of Industrial Chemistry*, 5th ed.; Elvers, B., Hawkins, S., Eds.; VCH: Weinheim, Germany, 1996; Vol. A27, p 581.
(3) Block, J. Vitamins. In *Kirk-Othmer Encyclopedia of Chemical Technology*, 5th ed.; Seidel, S., Ed.; Wiley: Hoboken, NJ, 1996; Vol. 25, p 797.
(4) Carlson, L. A. *J. Intern. Med.* **2005**, *258*, 94–114.
(5) Gille, A.; Bodor, E. T.; Ahmed, K.; Offermarms, S. *Annu. Rev. Pharmacol. Toxicol.* **2008**, *48*, 79–106.
(6) Shimizu, S. Vitamins and Related Compounds: Microbial Production. In *Biotechnology: A Multi-Vol. Comprehensive Treatise*, 2nd completely rev. ed.; Rehm, H.-J., Reed, G., Puhler, A., Stadler, P. J. W., Eds.; VCH: Weinheim, Germany, 2001; Vol. 10, p 320.
(7) Weissermel, K.; Arpe, H.-J. *Industrial Organic Chemistry*, 4th ed.; Wiley-VCH: Weinheim, Germany, 2003.
(8) Cantarella, M.; Cantarella, L.; Gallifuoco, A.; Intellini, R.; Kaplan, O.; Spera, A.; Martínková, L. *Enzyme Microb. Technol.* **2008**, *42*, 222–229.
(9) Brittain, H. G. *Polymorphism in Pharmaceutical Solids*; Marcel Dekker: New York, 1999.
(10) Bernstein, J. *Polymorphism in Molecular Crystals*; Oxford University Press: Oxford, U.K., 2002.
(11) Hilfiker, R. *Polymorphism in the Pharmaceutical Industry*; Wiley-VCH: Weinheim, Germany, 2006.
(12) Martinho Simões, J. A.; Minas da Piedade, M. E. *Molecular Energetics*; Oxford University Press: New York, 2008.
(13) Canongia Lopes, J. N.; Cabral do Couto, P.; Minas da Piedade, M. E. *J. Phys. Chem. A* **2006**, *110*, 13850–13856.
(14) Lousada, C. M.; Pinto, S. S.; Canongia Lopes, J. N.; Piedade, M. F. M.; Diogo, H. P.; Minas da Piedade, M. E. *J. Phys. Chem. A* **2008**, *112*, 2977–2987.
(15) Picciochi, R.; Lopes, J. N. C.; Diogo, H. P.; Minas da Piedade, M. E. *J. Phys. Chem. A* **2008**, *112*, 10429–10434.
(16) Bernardes, C. E. S.; Piedade, M. F. M.; Minas da Piedade, M. E. *Cryst. Growth Des.* **2008**, *8*, 2419–2430.
(17) Marsh, K. N. *Recommended Reference Materials for the Realization of Physicochemical Properties*; IUPAC-Blackwell Scientific Publications: Oxford, U.K., 1987.
(18) Vora, P.; Menon, D.; Samtani, M.; Dollimore, D.; Alexander, K. *Instrum. Sci. Technol.* **2001**, *29*, 231–245.
(19) Bickerton, J.; Pilcher, G.; Altakhin, G. *J. Chem. Thermodyn.* **1984**, *16*, 373–378.
(20) Ribeiro da Silva, M. D. M. C.; Gonçalves, J. M.; Acree, W. E., Jr. *J. Chem. Thermodyn.* **2000**, *32*, 1071–1073.
(21) Sabbah, R.; Ider, S. *Can. J. Chem.* **1999**, *77*, 249–257.

(22) Menon, D.; Dollimore, D.; Alexander, K. S. *Thermochim. Acta* **2002**, *392*−*393*, 237–241.
(23) Jessup, R. S. *J. Res. Natl. Bur. Stand. (U. S.)* **1942**, *29*, 247–270.
(24) Sato-Toshima, T.; Kamaguchi, A.; Nishiyama, K.; Sakiyama, M.; Seki, S. *Bull. Chem. Soc. Jpn.* **1983**, *56*, 51–54.
(25) Di, Y. Y.; Shi, Q.; Tan, Z. C.; Sun, L. X. *Acta Chim. Sinica* **2007**, *65*, 1940–1946.
(26) Tan, Z. C. Private communication.
(27) Koch, W.; Holthausen, M. C. A. *Chemist's Guide to Density Functional Theory*, 2nd ed.; Wiley-VCH: Weinheim, Germany, 2002.
(28) Curtiss, L. A.; Redfern, P. C.; Raghavachari, K.; Rassolov, V.; Pople, J. A. *J. Chem. Phys.* **1999**, *110*, 4703–4709.
(29) Montgomery, J. A., Jr.; Frisch, M. J.; Ochterski, J. W.; Petersson, G. A. *J. Chem. Phys.* **1999**, *110*, 2822–2827.
(30) Montgomery, J. A., Jr.; Frisch, M. J.; Ochterski, J. W.; Petersson, G. A. *J. Chem. Phys.* **2000**, *112*, 6532–6542.
(31) Laugier, J.; Bochu, B. *Chekcell*; http://www.ccp14.ac.uk/tutorial/lmgp/chekcell.htm.
(32) NIST Certificate for Standard Reference Material 2151.
(33) Taylor, L. D. *J. Org. Chem.* **1962**, *27*, 4064–4065.
(34) Goher, M. A. S.; Drátovský, M. *Collect. Czech. Chem. Commun.* **1975**, *40*, 26–35.
(35) Hudson, M. R.; Allis, D. G.; Hudson, B. S. *Chem. Phys. Lett.* **2009**, *473*, 81–87.
(36) Saito, T.; Hayamizu, K.; Yanagisawa, M.; Yamamoto, O.; Wasada, N.; Someno, K.; Kinugasa, S.; Tanabe, K.; Tamura, T.; Hiraishi, J. *Spectral Database for Organic Compounds (SDBS)*; http://riodb01.ibase.aist.go.jp/sdbs/.
(37) Moura Ramos, J. J.; Taveira-Marques, R.; Diogo, H. P. *J. Pharm. Sci.* **2004**, *93*, 1503–1507.
(38) Pinto, S. S.; Diogo, H. P.; Minas da Piedade, M. E. *J. Chem. Thermodyn.* **2003**, *35*, 177–188.
(39) Calado, J. C. G.; Dias, A. R.; Minas da Piedade, M. E.; Martinho Simões, J. A. *Rev. Port. Quim.* **1980**, *22*, 53–62.
(40) Diogo, H. P.; Minas da Piedade, M. E.; Fernandes, A. C.; Martinho Simões, J. A.; Ribeiro da Silva, M. A. V.; Monte, M. J. S. *Thermochim. Acta* **1993**, *228*, 15–22.
(41) Diogo, H. P.; Minas da Piedade, M. E.; Gonçalves, J. M.; Monte, M. J. S.; Ribeiro da Silva, M. A. V. *Eur. J. Inorg. Chem.* **2001**, *228*, 257–262.
(42) Kiyobayashi, T.; Minas da Piedade, M. E. *J. Chem. Thermodyn.* **2001**, *33*, 11–21.
(43) Bernardes, C. E. S.; Santos, L. M. N. B. F.; Minas da Piedade, M. E. *Meas. Sci. Technol.* **2006**, *17*, 1405–1408.
(44) Becke, A. D. *J. Chem. Phys.* **1993**, *98*, 5648–5652.
(45) Lee, C.; Yang, W.; Parr, R. G. *Phys. Rev. B* **1988**, *37*, 785–789.
(46) Mclean, A. D.; Chandler, G. S. *J. Chem. Phys.* **1980**, *72*, 5639–5648.
(47) Frisch, M. J.; Pople, J. A.; Binkley, J. S. *J. Chem. Phys.* **1984**, *80*, 3265–3269.
(48) Dunning, T. H. *J. Chem. Phys.* **1989**, *90*, 1007–1023.
(49) Dunning, T. H.; Peterson, K. A.; Wilson, A. K. *J. Chem. Phys.* **2001**, *114*, 9244–9253.
(50) Kendall, R. A.; Dunning, T. H.; Harrison, R. J. *J. Chem. Phys.* **1992**, *96*, 6796–6806.
(51) Frisch, M. J.; Trucks, G. W.; Schlegel, H. B.; Scuseria, G. E.; Robb, M. A.; Cheeseman, J. R.; Montgomery, J. A., Jr.; Vreven, T.; Kudin, K. N.; Burant, J. C.; Millam, J. M.; Iyengar, S. S.; Tomasi, J.; Barone, V.; Mennucci, B.; Cossi, M.; Scalmani, G.; Rega, N.; Petersson, G. A.; Nakatsuji, H.; Hada, M.; Ehara, M.; Toyota, K.; Fukuda, R.; Hasegawa, J.; Ishida, M.; Nakajima, T.; Honda, Y.; Kitao, O.; Nakai, H.; Klene, M.; Li, X.; Knox, J. E.; Hratchian, H. P.; Cross, J. B.; Adamo, C.; Jaramillo, J.; Gomperts, R.; Stratmann, R. E.; Yazyev, O.; Austin, A. J.; Cammi, R.; Pomelli, C.; Ochterski, J. W.; Ayala, P. Y.; Morokuma, K.; Voth, G. A.; Salvador, P.; Dannenberg, J. J.; Zakrzewski, V. G.; Dapprich, S.; Daniels, A. D.; Strain, M. C.; Farkas, O.; Malick, D. K.; Rabuck, A. D.; Raghavachari, K.; Foresman, J. B.; Ortiz, J. V.; Cui, Q.; Baboul, A. G.; Clifford, S.; Cioslowski, J.; Stefanov, B. B.; Liu, G.; Liashenko, A.; Piskorz, P.; Komaromi, I.; Martin, R. L.; Fox, D. J.; Keith, T.; Al-Laham, M. A.; Peng, C. Y.; Nanayakkara, A.; Challacombe, M.; Gill, P. M. W.; Johnson, B.; Chen, W.; Wong, M. W.; Gonzalez, C.; Pople, J. A. *Gaussian 03*, revision C.02; Gaussian, Inc.: Wallingford, CT, 2004.
(52) Jillavenkatesa, A.; Dapkunas, S. J.; Lum, L.-S. H. *Particle Size Characterization*; National Institute of Standards and Technology: Gaithersburg, MD, 2001.
(53) Kutoglu, A.; Scheringer, C. *Acta Crystallogr.* **1983**, *C39*, 232–234.
(54) Allen, F. H. *Acta Crystallogr.* **2002**, *B58*, 380–388.
(55) Macrae, C. F.; Edgington, P. R.; McCabe, P.; Pidcock, E.; Shields, G. P.; Taylor, R.; Towler, M.; van de Streek, J. *J. Appl. Crystallogr.* **2006**, *39*, 453–457.
(56) Wieser, M. E. *Pure Appl. Chem.* **2006**, *78*, 2051–2066.
(57) Gording, R.; Flexser, L. A. *J. Am. Pharm. Assoc.* **1940**, *5*, 230–231.
(58) Rehman, M.; Shekunov, B. Y.; York, P.; Colthorpe, P. *J. Pharm. Sci.* **2001**, *90*, 1570–1582.
(59) El Moussaoui, A.; Chauvet, A.; Masse, J. *J. Therm. Anal.* **1993**, *39*, 619–632.
(60) Wang, S. X.; Tan, Z. C.; Di, Y. Y.; Xu, F.; Wang, M. H.; Sun, L. X.; Zhang, T. *J. Therm. Anal. Calorim.* **2004**, *76*, 335–342.
(61) Allan, J. R.; Geddes, W. C.; Hindle, C. S.; Orr, A. E. *Thermochim. Acta* **1989**, *153*, 249–256.
(62) Späth, E.; Spitzer, H. *Ber. Dtsch. Chem. Ges.* **1926**, *59B*, 1477–1486.
(63) Malaviolle, R.; Demaury, G.; Chauvet, A.; Terol, A.; Masse, J. *Thermochim. Acta* **1987**, *121*, 283–294.
(64) Jingyan, S.; Jie, L.; Yun, D.; Ling, H.; Xi, Y.; Zhiyong, W.; Yuwen, L.; Cunxin, W. *J. Therm. Anal. Calorim.* **2008**, *93*, 403–409.
(65) Hubbard, W. N.; Scott, D. W.; Waddington, G. In *Experimental Thermochemistry*; Rossini, F. D., Ed.; Interscience: New York, 1956; Vol. 1, Chapter 5.
(66) Månsson, M.; Hubbard, W. N. In *Experimental Chemical Thermodynamics*; Sunner, S., Månsson, M., Eds.; Pergamon Press: London, 1979; Vol. 1, Chapter 5.
(67) Johnson, W. H. *J. Res. Natl. Bur. Stand. (U. S.)* **1975**, *79A*, 425–429.
(68) Wagman, D. D.; Evans, W. H.; Parker, V. B.; Schumm, R. H.; Halow, I.; Bailey, S. M.; Churney, K. L.; Nuttall, R. L. *J. Phys. Chem. Ref. Data* **1982**, *11*, suppl. no. 2.
(69) Santos, L. M. N. B. F.; Silva, M. T.; Schröder, B.; Gomes, L. *J. Therm. Anal. Calorim.* **2007**, *89*, 175–180.
(70) Olofsson, G. *Assignment of Uncertainties; In Experimental Chemical Thermodynamics*; Sunner, S., Månsson, M., Eds.; Pergamon Press: London, 1979; Vol. 1, Chapter 6.
(71) Cox, J. D.; Wagman, D. D.; Medvedev, V. A. *CODATA Key Values for Thermodynamics*; Hemisphere: New York, 1989.
(72) Edwards, J. W.; Kington, G. L. *Trans. Faraday Soc.* **1962**, *58*, 1323–1333.
(73) Andrews, J. T. S.; Westrum, E. F., Jr.; Bjerrum, N. *J. Organomet. Chem.* **1969**, *17*, 293–302.
(74) Atkins, P. W.; de Paula, J. *Physical Chemistry*, 7th ed.; Oxford University Press: Oxford, U.K., 2002; p 822.
(75) Pascual-Ahuir, J. L.; Silla, E.; Tunon, I. *GEPOL93*; http://www.ccl.net/cca/software/SOURCES/FORTRAN/molecular_surface/gepol93/.
(76) Bondi, A. *J. Phys. Chem.* **1964**, *68*, 441–451.
(77) Denbigh, K. *The Principles of Chemical Equilibrium*, 4th ed.; Cambridge University Press: Cambridge, U.K., 1981.
(78) Korn, G. A.; Korn, T. M. *Mathematical Handbook for Scientists and Engineers*; McGraw-Hill: New York, 1968.
(79) Irikura, K. K.; Frurip, D. J. *Computational Thermochemistry. Prediction and Estimation of Molecular Thermodynamics*; ACS Symposium Series No. 677; American Chemical Society: Washington, DC, 1998.
(80) Computational Chemistry Comparison and Benchmark DataBase. *NIST Standard Reference Database 101 (Release 12)*; National Institute of Standards and Technology: Gaithersburg, MD, 2005.
(81) Pedley, J. B. *Thermochemical Data and Structures of Organic Compounds*; TRC: College Station, TX, 1994; Vol. 1.

JP101490B